

COMMISSARIAT A L'ENERGIE ATOMIQUE

CENTRE D'ETUDES NUCLEAIRES DE SACLAY

Service de Documentation

F91191 GIF SUR YVETTE CEDEX

CEA-CONF - -8046

L9

A MULTIPLEX CODING IMAGING SPECTROMETER FOR X-RAY  
ASTRONOMY

ROCCHIA, R.; DESCHAMPS, J.Y.; KOCH-MIRAMOND, L.; TARRIUS, A.

CEA CEN Saclay, Service d'Astrophysique

Communication présentée à : Workshop on X-ray spectroscopy  
Lyngby (Denmark)  
24-26 Jun 1985

# A MULTIPLEX CODING IMAGING SPECTROMETER FOR X-RAY ASTRONOMY

R. Rocchia, J.Y. Deschamps, L. Koch-Miramond, A. Tarrus

Service d'Astrophysique, Centre d'Etudes Nucléaires de Saclay  
91191 Gif-sur-Yvette, Cedex, France

## ABSTRACT

The paper describes a multiplex coding system associated with a solid state spectrometer Si(Li) designed to be placed at the focus of a grazing incidence telescope. In this instrument the spectrometric and imaging functions are separated. The coding system consists in a movable mask with pseudo randomly distributed holes, located in the focal plane of the telescope. The pixel size lies in the range 100-200 microns. The close association of the coding system with a Si (Li) detector gives an imaging spectrometer combining the good efficiency (50% between 0,5 and 10 keV) and energy resolution ( $\Delta E \sim 90$  to 160 eV) of solid state spectrometers with the spatial resolution of the mask. Simulations and results obtained with a laboratory model are presented.

counters without imaging property. In that case the image can still be analyzed provided the signal of each pixel is time modulated by a coding function generated by a mobile mask. The photon detector output is the sum of the modulated signal of each pixel. The simplest image coding system is the ordinary spot scan (or pixel by pixel) analysis with an opaque mask equipped with a single hole (figure 1). The mask is moved step by step at regular time intervals in the plane of the image, (the focal plane of the X-ray telescope) so that the signal of one pixel at a time is collected by the detector located behind the mask. For an image consisting in M pixels, explored in a time T, a short time  $T/M$  is dedicated to a particular pixel and a small fraction only of the available signal is used. This is a bad situation in X-ray astronomy where the rule is to analyse low luminosity images.

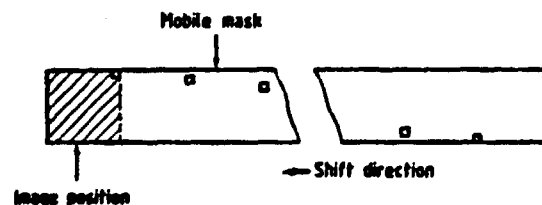


Figure 1. Mask for a spot-scan analysis

## 1. INTRODUCTION

Astronomical observations in the X-ray range with grazing incidence telescopes require focal plane imaging detectors. The most commonly envisaged imagers (proportional counters, gas scintillating counters, channel multiplier arrays, CCDs) are characterized by rather poor spectral capabilities. Even CCDs, in spite of an impressive improvement of performances achieved lately (Refs. 1,2) cannot yet compete, on a spectral ground, with single solid state spectrometers like the Si(Li) detectors (Ref. 3). However these Si(Li) detectors are devoided of any imaging capability. It is the purpose of this paper to describe an image coding system which, when associated with a non imaging spectrometer, provides an instrument combining the spectral resolution of the silicon spectrometer with the spatial resolution of the coder.

## 2. METHOD

The analysis of an image consists in determining the photon source strength of each portion of the image, which for convenience is divided into finite size picture elements (pixels). Usually the analysis is done with position sensitive detectors designed to determine the interaction place of the incident photons. In some cases such imaging devices are not available, or it is more convenient, for specific reasons, to use flux or photon

A more efficient way is to observe several pixels simultaneously: this is the so-called multiplex or area scan analysis. It can be shown that the technique, formerly proposed for infrared applications, results in a significant improvement of the signal to noise ratio (Refs. 4,5,6). This advantage must be paid for: the image restoration is not straightforward, a rather non trivial reconstruction process is required. On the other hand the impact position is not determined for each individual photon but statistically reconstructed for the whole set of photons recorded during the image observation. The coding operation is still achieved by the motion of a mask, but the transmission pattern is far more complex than the one used for the spot-scan analysis. For a given position of the mask the photon detector integrates information from a great number of pixels during a time  $\tau$ . Then the mask is shifted and a new group of pixels is observed. The signal of each pixel is time modulated by a series of 0's and 1's representing the transmission of the mask. The resulting modulating functions must be linearly independent. This is a necessary condition to make the deconvolution possible. The way the system works for a one dimensional image is obvious and the extension to a two-dimensional geometry

is straightforward (Ref. 4). For instance the mask shown on figure 2 consists of a chain of more or less rectangular patterns with the elements of each successive rectangle cyclically permuted by one row. The procedure is equivalent to the scan of a one dimensional picture generated by placing the rows of the picture end to end. The basic two-dimensional pattern is obtained by folding the initial coding function in the same way.

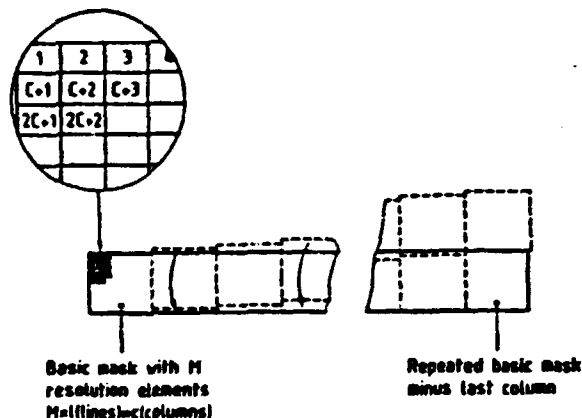


Figure 2. Mask for multiplex analysis of a bidimensional image

### 2.1 The coding functions

Cyclic binary functions are naturally adapted for the desired coding operation which is achieved by shifting a reticle. Purely random binary distributions could be used (Ref. 7) but distributions derived from pseudo noise functions have the advantage of an auto-correlation functions with perfectly flat side lobes. In the following we limit our considerations to functions having an average transmission  $(M-1)/2M$  (where  $M$  is the rank of the binary sequence = the number of pixels) like those proposed by Gottlieb (Ref. 4) and Girard (Ref. 5). But, in a general discussion the optimum coding function, depending on the complexity of the analyzed image (Refs. 6,8) should be chosen in a more general class of pseudo-random functions (see Refs. 9,10).

### 2.2. Coding

The reticle basic pattern is supposed to have the same dimension as the explored image. It is located in the focal plane of the X-ray telescope (figure 3). The photon detector is located behind it at a minimum distance to avoid the loss of photons due the beam divergence. The image exploration is done in a time  $T$  divided in  $M$  (number of pixels) exposures of duration  $\tau = T/M$  for each position of the mask. During the  $i^{th}$  exposure a number  $N_i$  of photons is detected. When the exploration is completed a set of  $M$  values  $N_i$  ( $i = 1, 2, \dots, M$ ) has been recorded: it constitutes the coded signal or vector  $\vec{N}$ .

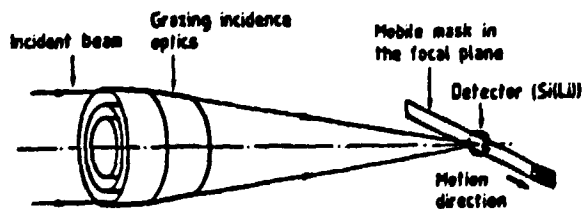


Figure 3. Multiplex coding system associated with a grazing incidence optics

### 2.3 Decoding

Two decoding methods have been used:

- the classical matrix inversion. The estimation  $\bar{m}$  of the image surface brightness is given by  $\bar{m} = [C]^{-1} \vec{N}$  where  $[C]$  is the coding matrix whose each line is obtained from the basic coding function by a cyclical permutation. The detector background supposed to be steady all over the observation is restored as a uniform increase of the surface brightness.

- the maximum entropy method which maximizes the quantity  $\sum m_i \ln(m_i)$  compatible with a normal statistical dispersion ( $\chi^2 \approx$  the number of degrees of freedom) and with the observed image total brightness ( $\sum N_i = (M-1)/2 \sum m_i$  for a reticle transparency of  $\frac{1}{2}$ ). Introducing the Lagrange multipliers we have to maximize the quantity:

$$Q(\mu, \nu) = - \sum_i m_i \ln(m_i) + \mu \sum_i (N_i - \sum_j c_{ij} m_j)^2 / N_i + \nu \sum_i m_i$$

where  $c_{ij}$  is the term of the coding matrix  $[C]$ .

### 3. SIMULATIONS

Computer simulations were carried out with a 63 pixel image. The mask was assumed to be perfect with 0 or 1 transmission value. Two examples are shown: an empty field and a point source.

#### 3.1 Empty field (Fig.4).

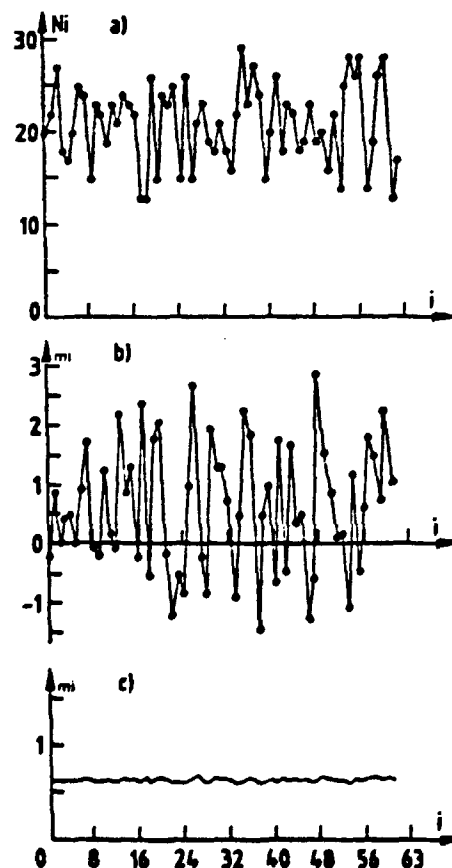


Figure 4. Computer simulation of a flat field.  
4a - Coded signal (detector background 1200 counts)  
4b - matrix inversion result  
4c - maximum entropy deconvolution  
The bidimensional image (9x7 pixels) is linearly displayed (line after line)

The counts are due to the detector background only. We have simulated an exposure of  $10^5$  seconds in an energy range of 120 eV (typical value of the energy resolution of a Si(Li) detector at 1 keV) with a 6mm diameter detector having a flat background of  $1\text{c s}^{-1}$  between 1 and 10 keV. Figure 4a shows the simulated signal Ni accumulated over a single or multiple scan of the field. On figure 4b we have plotted in a linear display (line after line) the image surface brightness obtained by matrix inversion. Figure 4c illustrates the smoothing effect of the maximum entropy method.

### 3.2 Point source (Fig. 5).

In addition to the detector background we have introduced a point source (pixel 32) corresponding to a 3 micro crab source observed with a  $10^3\text{cm}^2$  telescope in a range of 120 eV centered on 1 keV. One will note the absence of ghost image on figure 5 b and c. As expected the source intensity obtained by the maximum entropy method (which provides the minimum contrasted field compatible with the data) is much lower than the value obtained by matrix inversion (by a factor 3).

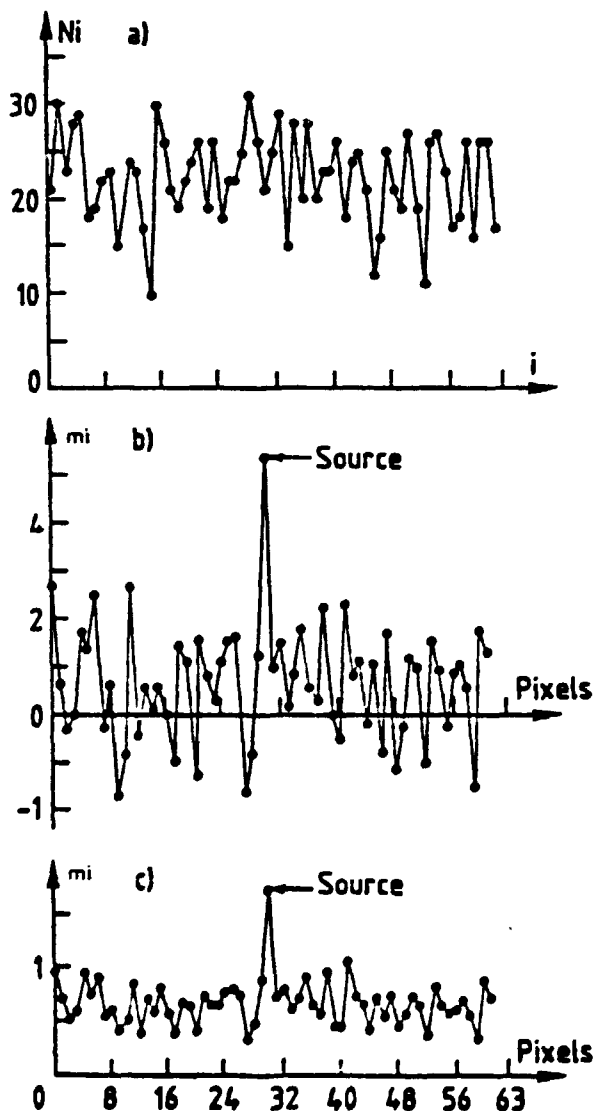


Figure 5. Same as figure 4 for a point source (150 counts) on a flat field (1200 counts). This simulation corresponds to a  $10^5$  seconds observation of a 3 micro-Crab source with a  $10^3\text{cm}^2$  telescope.

## 4. LABORATORY MODEL

### 4.1 Design

In order to evaluate the difficulty to implement such a device we have manufactured a mask of 1023 pixels of  $200 \times 200$  microns<sup>2</sup>. To simplify the step by step motion system and to avoid the code reset required before any analysis, we have preferred a ring shape geometry instead of a linear one (Fig. 6). The consequence is that the basic pattern and the pixel shape is slightly fan-shaped. The image is divided into 31x33 pixels and the reticle consists in a code of 33 lines followed by a full aperture (for full field observation) and a complete occultation zone (for detector background estimation) repeated twice. A complete rotation of the reticle allows two successive image explorations.

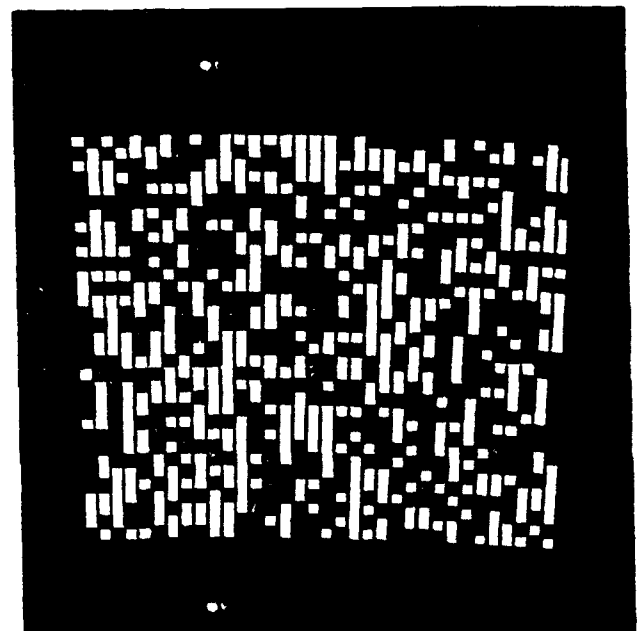
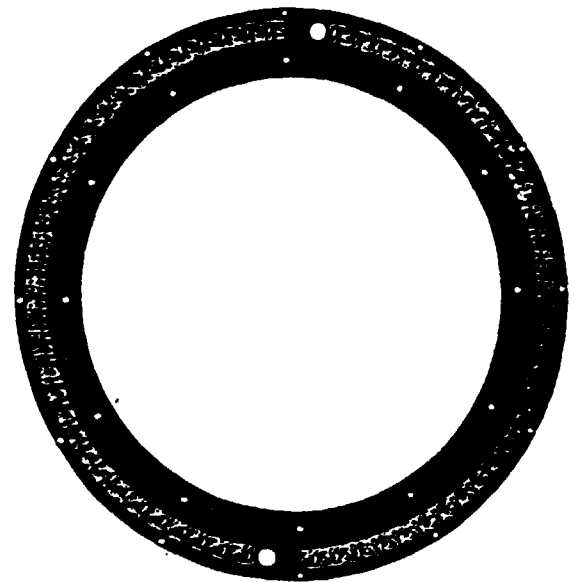


Figure 6. Ring shaped mask  
a - overall view  
b - detail of the code

#### 4.2 Manufacturing and mounting

The mask is made of nickel and was manufactured by electrodeposition with a thickness of 40 microns, value which guarantees a good absorption (98% at 6 keV) and a correct mechanical stiffness. The mask elements ( $200 \times 200 \mu^2$ ) are separated by a warp and weft structure 30 micron wide which increases the total opacity of the reticle (nominal value  $\approx 50\%$ ) to about 58%. The manufacturing accuracy (a few microns) of the mask and the mounting tolerances result in a radial clearance and a out-of-roundness lower than 15 microns. The mask is worked by a step by step motor but a continuous motion could also be used. Manoeuvres and data acquisition are controlled by a small computer.

For the laboratory tests we have used a proportional counter, equipped with a beryllium window slightly smaller than the basic image pattern, and located less than 1cm. behind the code. A fixed screen, with perforations of appropriate shapes, located 1mm in front of the mask simulates the X-ray images to be analyzed. X rays are produced by a  $^{56}\text{Fe}$  source.

#### 4.3 Results

Here again we present in a linear display, line by line, the bidimensional images reconstructed by matrix inversion only.

- "Point" source ( $\phi = 100 \mu$ , Fig. 7).

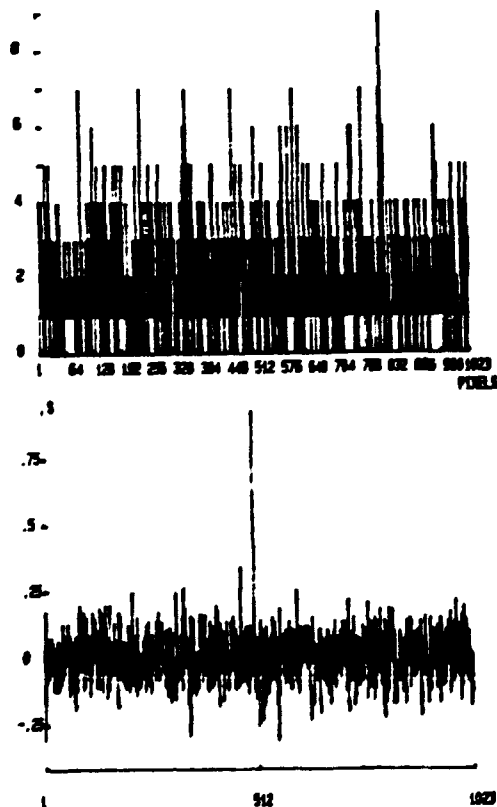


Figure 7. Observation of a point source ( $\phi = 100\text{microns}$ ) with the laboratory model  
7a - coded signal  
7b - matrix inversion result (linear display)  
The observation is equivalent to a space observation of a 25 micro-Crab source with a  $10^3 \text{ cm}^2$  telescope in  $5 \cdot 10$  seconds.

We have simulated the observation of a 25 micro-Crab in  $5 \cdot 10^4 \text{ s}$ . The source was positioned around pixel n° 503. The source is reconstructed at the right place (to one pixel) but with a brightness lower ( $11 \sigma$ ) than expected ( $25 \sigma$ ) (Fig. 7). This can be easily explained by the fact that the source was not initially perfectly centered on a pixel: the restored signal is spread over several adjacent pixels. In addition the absorption by the warp and weft structure significantly decreases the source signal.

- Extended source ( $\phi = 1\text{mm}$ ) giving a uniform brightness over an area equivalent to 18 pixels. The accumulated counts (fig.8a) simulate the observation of 1 milli-Crab source in  $10^5$  seconds with a  $10^3 \text{ cm}^2$  telescope.

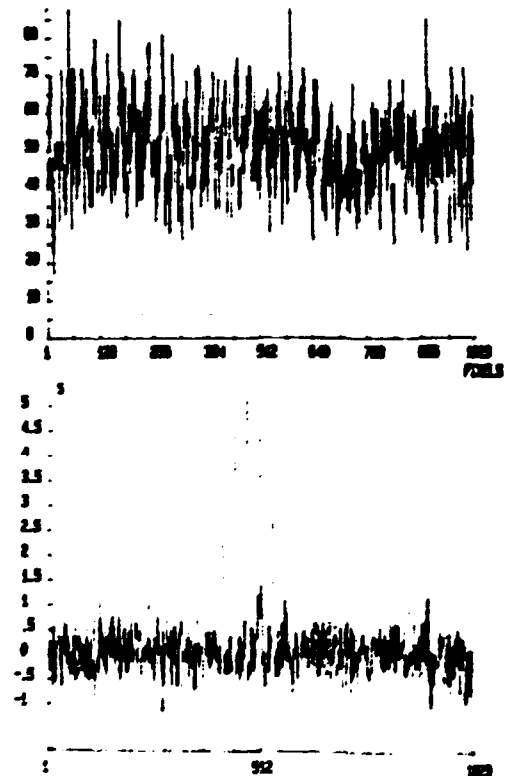


Figure 8. Same as figure 7 for an extended source ( $\phi = 1\text{mm}$ ) of 1 millicrab (50 micro-Crab per pixel)

The source is again perfectly reconstructed (Fig.8b) and located at the right place. The bidimensional plot (Fig.9) clearly shows that the shape of the image is properly restored. For the same reason as above the central brightness is a bit lower than expected. Of course, the edge could be more precisely reconstructed with smaller pixels and a continuous motion of the mask.

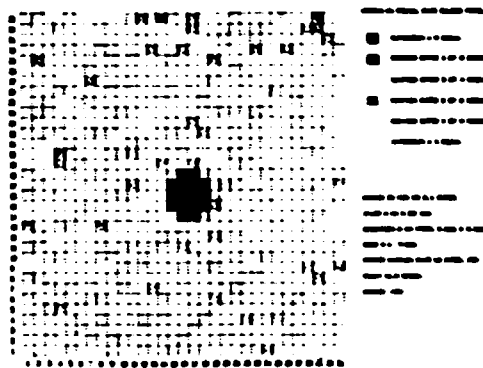


Figure 9. Bidimensional display of figure 8b.

## 6. CONCLUSIONS AND FUTURE PROSPECTS

We have presented results which show that the multiplex image coding system associated with a non-imaging detector can be efficiently used to analyze the X-ray image obtained at the focus of a grazing incidence telescope. The spatial information is recovered via the time distribution of the recorded events. This time is measured independently of the amplitude of each event and, thus, no interference between the spectrometric and imaging functions is foreseen. In other words independent images can be obtained in energy bandwidth equal to the energy resolution of the spectrometer. The association of the system with a cooled solid-state spectrometer (Si(Li)) would result in an excellent imaging spectrometer combining the spatial resolution of the coding system (200 microns in the present work) and the energy resolution of the solid state detector ( $\leq 100$  eV below 1 keV, 160 eV at 6 keV).

Our future program of work includes:

- Attempts to remove the warp or/and wett structures in order to reduce the dead area of the coder.
- Manufacturing of masks with pixels of  $100 \times 100$  (microns)<sup>2</sup>
- Development of interfaces with a cooled detector in order to minimize the thermal budget of the system. This point is critical for the lifetime of a space experiment.
- An optimum choice of the field effect transistor which constitutes the first stage of the Si (Li) preamplifier and which is the critical part determining the energy resolution at low energy.
- Investigations of the possibility to associate the coding system with a bolometer, if such detectors, whose size could be as large as  $1 \text{ mm}^2$ , can be used as X ray spectrometers (Refs. 11,12).

## 7. REFERENCES

1. Lumb D H et al , Center for Astrophysics, Preprint series n° 2131
2. Janesick J R et al, Rev.Sci.Inst. (to be published)
3. Musket R G 1974, Nucl. Inst. Meth., 117, 385-384.
4. Gottlieb P 1968, IEEE Trans. In. Theory 1, 14- 428.
5. Girard A 1971, in J.B. Lomax (ed.), AGARD Conf. Proceedings, CP-90, N° 33.
6. Rocchia R et al 1983, Astrophysics and Space Science 96, 361-374.
7. Dicke R H 1968, Astrophys.J. 153, L101.
8. Koral K F et al 1975, J. Nucl. Medicine 16, N°5, 402.
9. Hossfeld F & Amadori R 1970, Kernforschungsanlage Jülich Report, Jul. 684 FF.
10. Wilhelmi G 1970, Kernforschungszentrum Karlsruhe Report KFK-1177.
11. Moseley S H et al 1985, IEEE Trans. Nucl. Science. NS-32. 134-138.
12. Coron N et al 1985, Nature, 314, 75-76.